Fully relativistic study of forbidden transitions of O II: Electron density diagnosis for planetary nebulas

Shaohao Chen,[1] Bo Qing,[1] and Jiaming Li[2,1]
[1]*Key Laboratory of Atomic and Molecular Nanosciences of Education Ministry, Department of Physics, Tsinghua University, Beijing 100084, China*
[2]*Department of Physics, Shanghai Key Laboratory for Laser Fabrication and Material Science, Shanghai Jiaotong University, Shanghai 200030, China*
(Received 9 April 2007; published 10 October 2007)

Using the multiconfiguration Dirac-Fock method, including the quantum electrodynamics corrections, especially with the Breit interactions, we calculate the electric quadrupole ($E2$) and magnetic dipole ($M1$) transition rates for the two transitions $^2D^o_{5/2,3/2} \rightarrow {}^4S^o_{3/2}$ of O II. We show systematically that the correlation effects owing to core electron excitations and the Breit interactions are vitally important for the transition rates. We present a benchmark for the intensity ratio between the two transitions in the limit of high electron density in planetary nebulas, i.e., $r(\infty)=0.345^{+0.028}_{-0.014}$, which is in good agreement with modern astronomical observations.

DOI: 10.1103/PhysRevA.76.042507 PACS number(s): 32.10.−f, 32.70.−n, 95.30.Ky

Singly ionized oxygen (O II) is of great interest in astronomy and astrophysics. A knowledge of the intensity ratio $I(3729)/I(3726)$, i.e., the ratio between the two transitions $^2D^o_{5/2,3/2} \rightarrow {}^4S^o_{3/2}$, can be used to diagnose the electron densities in planetary nebulas (PNs) [1]. In the limit of high electron density, the detailed balance between collisional excitations and deactivations leads to a Boltzmann distribution. Since the splitting of ^2D (about 20 K) is much lower than the electron temperature in typical PNs ($T_e > 1000$ K), the line intensities are proportional to the radiative transition rates and the statistical weights of ionic levels. In the limit of low electron density, the line intensities are proportional to the collision strengths, because of the equilibrium between the radiative transitions and the collisional excitations. In this paper, we focus on the intensity ratio in the limit of high electron density. The transitions $^2D^o_{5/2,3/2} \rightarrow {}^4S^o_{3/2}$ are forbidden for electric dipole ($E1$) radiations; hence the total transition rates are dominated by electric quadrupole ($E2$) and magnetic dipole ($M1$) radiations, which are delicate to calculate. We use the GRASP code [2] based on the multiconfiguration Dirac-Fock (MCDF) method [3,4] to calculate the $E2$ and $M1$ transition rates. These calculations are fully relativistic, taking into account large-scale electron correlations, including the quantum electrodynamics (QED) corrections as perturbations, in particular with the Breit interactions. In earlier work, the importance of the two-electron Breit terms (in the Breit-Pauli order) on the $M1$ transition rates of O II was investigated by Eissner and Zeippen [5]. Extensive correlation effects were investigated in the calculations of Fischer and Tachiev [6,7], and the importance of the core-excitation correlations in $E1$ transition rates of heavy elements was investigated by Zou and Fischer [8]. In this paper, we systematically investigate the importance of the core-excitation correlations and the Breit interactions in the $E2$ and $M1$ transition rates of O II. Finally, we present a benchmark value for the intensity ratio in the limit of high electron density, i.e., $r(\infty)=0.345^{+0.028}_{-0.014}$. Our calculated ratio is in good agreement with the astronomical observations by Wang and Liu [9], Monk [10], and Copetti [11], and also agrees well with an earlier calculation result (0.348) by Zeippen [12], but disagrees with later calculation results 0.297 by Zeippen [13] and 0.26 by Wiese [14].

We first present a brief summary of the MCDF method and our calculation strategies. The interactions in atomic systems can be separated into two parts: longitudinal and transverse interactions. In the Coulomb gauge, the atomic Hamiltonian with a potential including the longitudinal electron-nucleus and electron-electron interactions, i.e., the Dirac-Coulomb Hamiltonian, can be expressed as (atomic units are adopted in this paper),

$$H_{DC} = \sum_i \left(c\vec{\alpha} \cdot \vec{p}_i + (\beta - 1)c^2 - \frac{Z}{r_i} \right) + \sum_{i<j} \frac{1}{|\vec{r}_i - \vec{r}_j|}. \quad (1)$$

The transverse interactions and the interactions with radiation fields can be treated as perturbations, which will be presented later. The full relativistic atomic orbital (AO) wave functions are obtained by solving the Dirac-Fock equations self-consistently, i.e.,

$$H_{DC}\psi = E\psi. \quad (2)$$

Important electron correlation effects are taken into account to optimize the AOs through multiconfiguration self-consistent-field (MCSCF) iterations. More specifically, the AOs with principal quantum numbers $n \leqslant 3$ are optimized together by MCSCF iterations, in order to take into account the correlations including $3s$, $3p$, and $3d$ orbitals. The

TABLE I. The calculation strategies for the AO sets. (V, excitations from the valence $2s^2 2p^3$; C, excitations from the core $1s^2$; S, single excitations; D, double excitations.)

	n				
	$\leqslant 3$	4	5	6	7
Set 1	V+C; S+D	V+C; S	V+C; S	V; S+D	V; S+D
Set 2	V+C; S+D	V+C; S+D	V+C; S+D	V; S+D	V; S+D
Set 3	V+C; S+D	V+C; S+D	V+C; S	V; S+D	V; S+D
Set 4	V; S+D	V; S	V; S		

TABLE II. The fine-structure energy levels of the ground configuration of O II ($1s^2 2s^2 2p^3$) (in atomic units).

Term	Present[a]	Expt.[b]	Difference[c]	Calc.[d]
$^4S^o_{3/2}$	0	0		0
$^2D^o_{5/2}$	0.122850	0.122158	0.57%	0.123129
$^2D^o_{3/2}$	0.122941	0.122249	0.57%	0.123219
$^2D^o_{5/2}$-$^2D^o_{3/2}$	−0.000091	−0.000091		−0.000090
$^2P^o_{3/2}$	0.184793	0.184384	0.22%	0.184877
$^2P^o_{1/2}$	0.184806	0.184393	0.22%	0.184889
$^2P^o_{3/2}$-$^2P^o_{1/2}$	−0.000012	−0.000009		−0.000012

[a]Present work.
[b]Experiment by Wenåker [18].
[c]Percentage difference between results of present work and [18].
[d]Calculation by Tachiev and Fischer [6].

valence-valence (VV), core-valence (CV), and core-core (CC) correlations are taken into account for sets 1, 2, and 3, i.e., the configurations are generated by single (S) and double (D) electron excitations from the core (C) $1s^2$ and the valence (V) $2s^2 2p^3$ orbitals. Only the VV correlations are taken into account for set 4, i.e., the core is fixed. With the above AOs ($n \leqslant 3$) fixed, we extend the AO sets to $n_{max}=4,5,6,7$ respectively. The calculation strategies for the four AO sets are described in Table I.

Configuration state functions (CSFs) are linear combinations of Slater determinants of the AOs with $n \leqslant n_{max}$. Atomic state functions (ASFs) are linear combinations of CSFs with the same parity (P), total angular momentum (J), and magnetic quantum number (M),

$$|\Gamma PJM; n_{max}\rangle = \sum_{r=1}^{n_c} C_{r\Gamma} |\gamma_r PJM; n_{max}\rangle, \tag{3}$$

where $C_{r\Gamma}$ is the mixing coefficient, and Γ, γ represent all other quantum numbers. Configuration interaction (CI) calculations including the S and D excitation configurations are carried out to obtain the atomic energy levels. The QED corrections, especially the Breit interactions, can be added to the atomic Hamiltonian in the CI calculations. The Breit interaction is the most important high-order correction in our calculations. The Breit (transverse) interaction represents the relativistic retardation effect of electromagnetic interactions with the finite velocity of light [15,16], especially the retarded magnetic interactions among the electron currents [17]. The calculated energy levels using sets 1, 2, and 3 are converged. The calculated energy levels using set 1 with $n_{max}=7$ including the Breit interactions are listed in Table II, compared with experimental [18] and other calculation results [6]. The differences between our calculation results and the experimental results are the smallest in the literature to our knowledge [6,19]. The small differences will not affect the errors in calculation of the transition rates.

The spontaneous radiative transition rate for a discrete transition $i \rightarrow j$ can be obtained as

$$A_{ij} = \frac{2\pi}{2J_i + 1} \sum_{M_i, M_j} |\langle \Gamma_j P_j J_j M_j | \mathbf{T}^{(k)}_{\lambda} | \Gamma_i P_i J_i M_i \rangle|^2, \tag{4}$$

where $\mathbf{T}^{(k)}_{\lambda}$ is the multipole radiation field operator. According to the Wigner-Eckart theorem, the transition matrix element is related to the reduced matrix element $\langle \Gamma_j P_j J_j \| \mathbf{T}^{(k)} \| \Gamma_i P_i J_i \rangle$. Substituting the ASFs by CSFs, and in turn by AOs, the reduced matrix element can be calculated by the sum of single-electron reduced matrix elements. In the Coulomb gauge, $\mathbf{T}^{(k)}$ has two forms: $\mathbf{T}^{(k)}(m)$ for magnetic fields and $\mathbf{T}^{(k)}_t(e)$ for electric fields. The Coulomb gauge corresponds to the velocity gauge in the nonrelativistic limit. In the length gauge, the electric multipole operator has another form $\mathbf{T}^{(k)}(e) = \mathbf{T}^{(k)}_t(e) + \sqrt{(k+1)/k}\,\mathbf{T}^{(k)}_l(e)$. The details are described elsewhere [20–22]. The electric transition rates calculated in the two gauges are the same for accurate wave

TABLE III. The $E2$ and $M1$ transition rates for $^2D^o_{5/2,3/2} \rightarrow {}^4S^o_{3/2}$ (in units of s^{-1}).

Transition	Type	Present[a]	Zeippen [12]	Zeippen [13]
$^2D^o_{5/2} \rightarrow {}^4S^o_{3/2}$	$E2$	$3.91^{+0.08}_{-0.11}(-5)$	3.64(−5)	3.39(−5)
	$M1$	$3.00^{+0.06}_{-0.06}(-6)$	1.83(−6)	1.98(−6)
	$E2+M1$	$4.21^{+0.09}_{-0.11}(-5)$	3.82(−5)	3.59(−5)
$^2D^o_{3/2} \rightarrow {}^4S^o_{3/2}$	$E2$	$3.48^{+0.20}_{-0.99}(-5)$	2.36(−5)	2.20(−5)
	$M1$	$1.48^{+0.01}_{-0.00}(-4)$	1.41(−4)	1.59(−4)
	$E2+M1$	$1.83^{+0.03}_{-0.10}(-4)$	1.65(−4)	1.81(−4)

[a]Our recommended transition rates and errors.

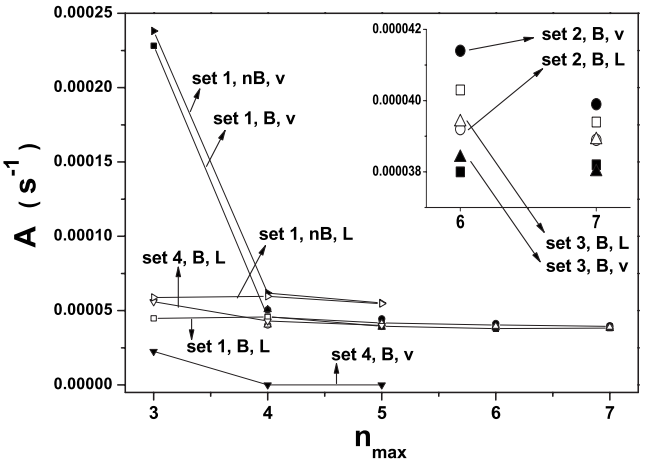

FIG. 1. $E2$ transition rates for $^2D^o_{5/2} \rightarrow {}^4S^o_{3/2}$. ■, set 1, B, V; □, set 1, B, L; ●, set 2, B, V; ○, set 2, B, L; ▲, set 3, B, V; △, set 3, B, L; ▼, set 4, B, V; ▽, set 4, B, L; ▶, set 1, nB, V; ▷, set 1, nB, L. The calculation strategies for the four AO sets are presented in Table I. B and nB, respectively, represent results including and not including the Breit interactions. V represents the velocity gauge, and L the length gauge.

functions; however, they are generally different in multiconfiguration calculations. Hence the quality of the wave functions can be tested by the gauge differences. In the velocity gauge, the electric transition rates depend sensitively on the wave functions at short distances, while in the length gauge they depend sensitively on the wave functions at long distances [20,21]. The magnetic transition rates depend sensitively on the wave functions at intermediate distances.

The calculated $E2$ transition rates for $^2D^o_{5/2} \rightarrow {}^4S^o_{3/2}$ with $3 \leqslant n_{max} \leqslant 7$ are plotted in Fig. 1. The $E2$ transition rates in the length gauge are much more stable and reliable than those in the velocity gauge. Using sets 1, 2, and 3, although the gauge differences are large with $n_{max}=3$, they become much smaller with $n_{max}=4$ and 5, indicating convergence. Using set 4 without core excitations, the gauge differences are still large with $n_{max}=4$ and 5, indicating that convergence

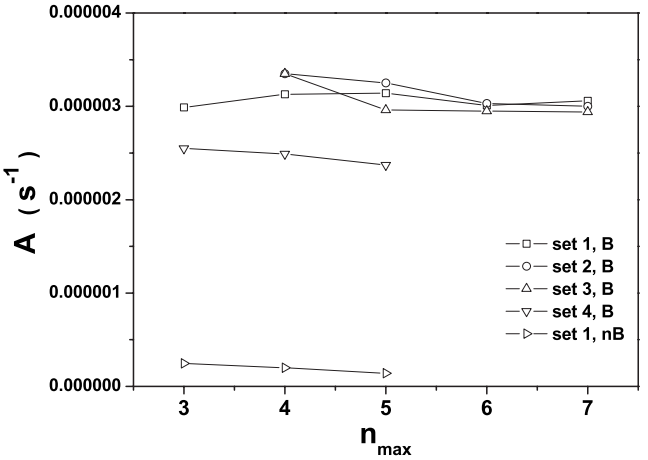

FIG. 2. $M1$ transitions rates for $^2D^o_{5/2} \rightarrow {}^4S^o_{3/2}$. The legends is the same as in Fig. 1. Note that the scale is larger than that in Fig. 1.

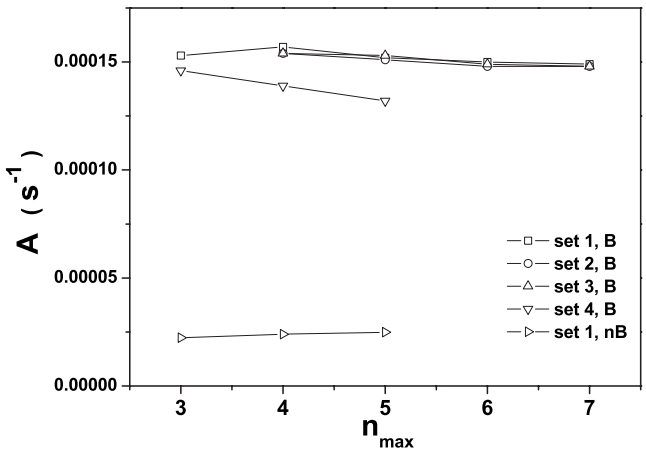

FIG. 3. $M1$ transitions rates for $^2D^o_{3/2} \rightarrow {}^4S^o_{3/2}$. The legend is the same as in Fig. 1.

is not achieved. More specifically, the core-excitation correlations drastically influence the wave functions at short distances; hence they are important for the convergence of the electric transition rates in the velocity gauge. The Breit interaction reduces the $E2$ transition rates by about 30% (as shown in Fig. 1). As sets 1, 2, and 3 enlarge, the gauge differences become smaller, and reach about 2% with $n_{max}=7$. In order to show the details, we insert an enlarged figure for $n_{max}=6,7$. The average of the $E2$ transition rates in the length gauge calculated using sets 1, 2, and 3 with $n_{max}=7$ is recommended as the final value, i.e., $3.91^{+0.08}_{-0.11} \times 10^{-5}$ s^{-1} (listed in Table III), with the positive (negative) error estimated by the difference between the average and the maximum (minimum) $E2$ transition rate in both gauges. The small gauge differences show that the wave functions are accurate enough at both short and long distances; hence they are also anticipated to be accurate at intermediate distances, which indicates that the calculated $M1$ transition rates for $^2D^o_{5/2} \rightarrow {}^4S^o_{3/2}$ (plotted in Fig. 2) are reliable. The $M1$ transition rates calculated using set 4 are smaller than those calculated using sets 1, 2, and 3, which shows that the core-excitation

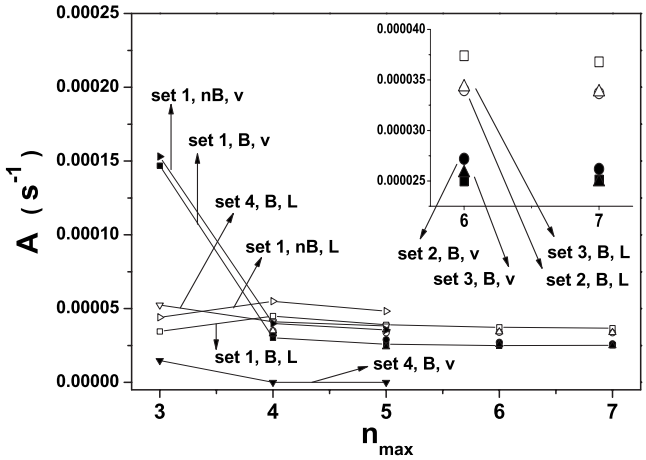

FIG. 4. $E2$ transitions rates for $^2D^o_{3/2} \rightarrow {}^4S^o_{3/2}$. The legend is the same as in Fig. 1.

TABLE IV. The intensity ratio between $^2D^o_{5/2} \rightarrow {}^4S^o_{3/2}$ and $^2D^o_{3/2} \rightarrow {}^4S^o_{3/2}$ at the high-electron-density limit.

	Present	Seaton [1]	Zeippen [12]	Zeippen [13]	Wiese [14]
Calculated $r(\infty)$	$0.345^{+0.028}_{-0.014}$	0.43	0.348	0.297	0.26
Observed $r(\infty)$		Monk [10] IC 418	Wang & Liu [9] H1-35		
		0.339±0.028	0.378±0.017		

correlations are also important for the magnetic transition rates. More specifically, they influence the wave functions at intermediate distances. The Breit interaction enhances the $M1$ transition rates by a factor of about 15 (as shown in Fig. 2), in particular, since it represents the retarded magnetic interaction of the electron currents. As the sets 1, 2, and 3 enlarge, the $M1$ transition rates are converging, with the recommended value $3.00^{+0.06}_{-0.06} \times 10^{-6}$ s^{-1}. The $E2$ transition rate is larger than the $M1$ transition rate by a factor of about 13; hence the calculation errors for the total transition rates mainly arise from the former (about 2%). Similarly, the $M1$ and $E2$ transition rates for $^2D^o_{3/2} \rightarrow {}^4S^o_{3/2}$ are plotted, respectively, in Figs. 3 and 4. The Breit interaction enhances the $M1$ transition rates by a factor of about 6 and reduces the $E2$ transition rates by about 30%. The gauge differences of the $E2$ transition rates reach about 25% with $n_{max}=7$; hence convergence is not completely achieved. Fortunately, the $E2$ transition rate (i.e., $3.48^{+0.20}_{-0.99} \times 10^{-5}$ s^{-1}) is smaller than the $M1$ transition rate (i.e., $1.48^{+0.01}_{-0.00} \times 10^{-4}$ s^{-1}) by a factor of about 4; hence the total transition rate is dominated by the latter, with the total errors only about 5%.

Our recommended transition rates and errors are listed in Table III, compared with other calculation results. In an earlier calculation in 1982 [12], a nonrelativistic Hamiltonian was adopted, only with relativistic corrections to the $M1$ transition operator, and a small AO set with $n_{max}=3$ and 4 was adopted, totally including only nine configurations. Hence the relativistic effects and especially the effect of the Breit interactions have not been fully taken into account and convergence may not be achieved. In a later calculation in 1987 [13], the AO set was enlarged to $n_{max}=4$, totally including 23 configurations, but may not be large enough to include all of the important electron correlations yet. In the present work, a full relativistic Hamiltonian is adopted, with the QED corrections especially the Breit interactions as perturbations, and the AO sets with $n_{max}=7$ include 39 777 configurations, with large-scale electron correlations, especially the core-excitation correlations taken into account. Hence the present work is more reliable. Using the total transition rates, the intensity ratio $I(3729)/I(3726)$ at the high electron density limit can be calculated as [1]

$$r(\infty) = \frac{6A_{E2+M1}(^2D^o_{5/2} \rightarrow {}^4S^o_{3/2})}{4A_{E2+M1}(^2D^o_{3/2} \rightarrow {}^4S^o_{3/2})}. \quad (5)$$

Our calculated intensity ratio and errors are listed in Table IV, compared with observations and other calculations. The astronomical observation work reported by Wang and Liu [9], Monk [10], and Copetti [11] all indicate that the ratio should be around 0.35. The observation results are based on hundreds of PNs, such as H1-35, IC4997, IC418, M1-64, NGC6833, etc. Our calculated ratio $0.345^{+0.028}_{-0.014}$ is in good agreement with the observations. Although the earlier calculated ratio 0.348 by Zeippen [12] is also supported by the observations, all of the transition rates are underestimated, as listed in Table III. The later calculated ratios 0.297 by Zeippen [13] and 0.26 by Wiese [14] are not supported by the observations.

Finally, we conclude with the following comments. Based on the multiconfiguration Dirac-Fock method including the QED corrections especially with the Breit interactions, we calculate the $E2$ and $M1$ transition rates for the transitions $^2D^o_{5/2,3/2} \rightarrow {}^4S^o_{3/2}$ of O II. We present a benchmark value for the intensity ratio $I(3729)/I(3726)$ in the limit of high electron density, i.e., $r(\infty)=0.345^{+0.028}_{-0.014}$, which should be interesting for astronomical observers.

This work is supported by the Ministry of Science and Technology and the Ministry of Education of China, the Key Grant Project of Chinese Ministry of Education (No. 306020), the National Natural Science Foundation of China, the National High-Tech ICF Committee in China, the Yin-He Super-computer Center, Institute of Applied Physics and Mathematics, Beijing, China, and the National Basic Research Program of China (Grant No. 2006CB921408). We would like to thank Liu XiaoWei for helpful discussions.

[1] M. J. Seaton and D. E. Osterbrock, Astrophys. J. **125**, 66 (1957).
[2] F. A. Parpia, C. F. Fischer, and I. P. Grant, Comput. Phys. Commun. **94**, 249 (1996).
[3] I. P. Grant, Adv. Phys. **19**, 747 (1970).
[4] J. P. Desclaux, Comput. Phys. Commun. **9**, 31 (1975).
[5] W. Eissner and C. J. Zeippen, J. Phys. B **14**, 2671 (1981).
[6] G. I. Tachiev and C. F. Fischer, Astron. Astrophys. **385**, 716 (2002).
[7] C. F. Fischer and Tachiev, At. Data Nucl. Data Tables **87**, 1 (2004).
[8] Y. Zou and C. F. Fischer, Phys. Rev. Lett. **88**, 183001 (2002).

[9] W. Wang, X. W. Liu, Y. Zhang, and M. Barlow, Astron. Astrophys. **873**, 886 (2004).
[10] D. J. Monk, M. J. Barlow, and R. E. S. Clegg, Mon. Not. R. Astron. Soc. **242**, 457 (1990).
[11] M. V. F. Copetti and B. C. Writzel, Astron. Astrophys. **382**, 282 (2002).
[12] C. J. Zeippen, Mon. Not. R. Astron. Soc. **198**, 111 (1982).
[13] C. J. Zeippen, Astron. Astrophys. **173**, 410 (1987).
[14] W. L. Wiese, J. R. Fuhr, and T. M. Deters, *Atomic Transition Probabilities of Carbon, Nitrogen, and Oxygen: A Critical Data Compilation* (American Chemical Society, Washington, DC, 1996).
[15] J. B. Mann and W. R. Johnson, Phys. Rev. A **4**, 41 (1971).
[16] I. P. Grant and B. J. McKenzie, J. Phys. B **13**, 2671 (1980).
[17] See I. P. Grant, *Relativistic Quantum Theory of Atoms and Molecules* (Springer-Verlag, New York, 2006), Secs. 4.9 and 10.11.
[18] I. Wenåker, Phys. Scr. **42**, 667 (1990).
[19] S. H. Chen, X. Y. Han, X. L. Wang, and J. M. Li, Chin. Phys. Lett. **24**, 1214 (2007).
[20] I. P. Grant, J. Phys. B **7**, 1458 (1974).
[21] Z. X. Zhao and J. M. Li, Acta Phys. Sin. **34**, 1769 (1985).
[22] K. G. Dyall *et al.*, Comput. Phys. Commun. **55**, 425 (1989).